Exploring heat and cold wave susceptible areas of India using consistency and frequency coupled novel approach

Rajesh Sarda
University of Gour Banga
Doli Halder
University of Gour Banga
Priyanka Das
Malda Women's College
Swades Pal (swadespal2017@gmail.com)
University of Gour Banga

Research Article

Keywords: Extreme temperature pattern, Hotspot analysis, Heat wave, Cold wave, and Heat and cold wave matrix

Posted Date: June 17th, 2022

DOI: https://doi.org/10.21203/rs.3.rs-1749917/v1

Exploring heat and cold wave susceptible areas of India using consistency and frequency coupled novel approach

Rajesh Sarda[1], Doli Halder[2], Priyanka Das[3], and Swades Pal[4]*

[1] Research Scholar, Department of Geography, University of Gour Banga, India. Email: rajeshsarda127@gmail.com

[2] PG student, Department of Geography, University of Gour Banga, India. Email: dolihaldar38@gmail.com

[3] Assistant Professor, Department of Geography, Malda Women's College, India. Email: priyankadas694@gmail.com

[4] Professor, Department of Geography, University of Gour Banga, India. Email: swadespal2017@gmail.com

*Corresponding author

Exploring heat and cold wave susceptible areas of India using consistency and frequency coupled novel approach

Abstract

A good many studies identified year-specific heat wave (HW) and cold wave (CW) using a percentile approach, the present study tried to identify and grade consecutive two and five days HW and CW spells using consistency and frequency coupled approach using the Indian Meteorological Department (IMD) endorsed gridded data across India since 1961 to 2021. The entire period was split into dry (1961-1990) and wet (1991-2021) phases to explore the long-term average of extreme temperature patterns and HW and CW change. The study revealed that wider parts of north western and central India were prone to statistically significant 30 years, 7 years, and 1-year average extreme temperature hot spot, and J & K and parts of north western India were prone to cold-spot (at 95 and 99% levels). The hot-spot and cold-spot dominated areas were again spotted as highly consistent and high-intensity HW and CW. About 60-65% area of north-western and central India was found consistent HW covering north western and central India. However, frequency and consistency coupled with HW intensity were recognized at five patches of the same area. Rajasthan and Delhi regions were found as the most intense HW zone. The average phase-wise change of HW was not very clear, however, some grids of this region recorded an increasing frequency of HW. CW intensity was increased by 13-26% in the northwestern tract over the phases. HW and CW matrix exhibited the co-existence of high intensity of HW and CW in the Rajasthan and Delhi region indicating high socio-ecological susceptibility. The findings of this study would be instrumental for regional priority planning and building adaptive capacity for combating the situation.

Keywords

Extreme temperature pattern, Hotspot analysis, Heat wave, Cold wave, and Heat and cold wave matrix

Introduction

The recent report of the Intergovernmental Panel on Climate Change (IPCC) has vividly stated that the consequences of climate change will direct to increasing extreme temperatures and the frequency of extreme temperature days (IPCC, 2013). This cruel truth has currently become progressively more obvious in different forms of extreme weather like increasing thermal anomaly, heat waves (HW) and cold waves (CW), and so on (Pai et al., 2017; Smid et al., 2019). IPCC (2007) reported increasing global mean temperature over the last 100 years (1906–2005) by 0.76 ± 0.18 °C.

The worldwide increase of HW and change in CW frequency has been considered one of the serious effects of climate change since the beginning of the 21st century. World Meteorological Organization (WMO, 2022) published a report made by a group of scientists on early HW occurrences 30 times more likely in India and Pakistan insists this concern. Some of the record-breaking HW incidents in recent times are HW in Southwestern Asia in late July and early August 2011, in California in June 2016, northwest India and Pakistan in May and June 2018, Indo-Pakistan HW (50.8°C) in 2019, in India, April 2022 (WMO, 2022). On the contrary, many parts of the world including India also experience CW at different times. The death toll of 8520 from 1978 to 2014 caused by 606 cold wave events clarifies the presence and intensity of CW in India (Malik et al., 2020). Malik et al. (2020) further reported that the frequency of CW and related mortality was found maximum in Central northeast and northwest meteorological regions from 1978 to 2014. Usually, during summer months (April, May, and June) India experiences HW events and during winter months (December, January) India faces CW incidents. Preceding works of literature in the context of the anticipated global warming and climate unpredictability, arraying from the global to regional scales, advocated that in coming decades the frequency and intensity of such HW events are likely to be enhanced (Sillmann et al., 2013; Russo et al., 2015; Dubey and Kumar, 2022). As per the Fifth report of IPCC (IPCC, 2013), the frequency and intensity of such extreme events may rise further, and densely populated Asian countries may be the worst victims.

Effects of such extreme events will not only affect the human physiological discomfort (Kumar et al., 2022) but also pose serious effects on ecology, agricultural and agro-industrial production systems, and thereby economy, infrastructure, and living beings across different parts of the world (Coumou and Rahmstorf, 2012; Lesk et al., 2016; Mishra, 2017; Rajkumar

et al., 2021; Azhar et al., 2022). Among the affected region, a wider part of India is seriously exposed to HW and CW risks (Azhar et al., 2022). This makes the situation highly vulnerable to economically marginal outdoor workers (WMO, 2022). More than 1.25 billion Indians are dependent on outdoor activities like the construction and agriculture sectors (Government of India, 2013). Particularly, in North India and Gangetic plain, the rice, wheat, and fruits production system, which warrants rural people's employment and the country's food security, is at high risk from such hot and cold spells (McCormick, 2012; Seneviratne et al., 2012; McCarl, 2013). So, extreme weathers like HW and CW are some major socio-ecological concerns (Bakhsh et al., 2018; Budhathoki et al., 2020; Raymond et al., 2020; Kumar and Singh, 2021). Considering this the present study tried to explore the changing extreme temperature pattern from 1960 to 2020.

So far the studies on extreme temperature analysis are concerned the researcher showed the distribution of temperature of some specific years in some specific part of India or as a whole or analyzing HW or CW. In very rare cases, statistical pattern analysis using long-term time series extreme temperature data over India is addressed. The present study tried to explore the pattern of extreme temperatures and their changes between dry (1961-1990) and wet (1991-2021) phases as defined by a report prepared by P. Guhathakurta and M. Rajeevan on "Trends in the rainfall pattern over India" and published by National Climate Centre (2006). They classified the entire period into four climatic regimes from 1901 to 2020. The 1961-1990 and 1991-2020 can be considered dry and wet phases based on rainfall anomalies. Since rainfall can reduce the temperature intensity, the present study is an axiom that in the wet phase extreme temperature intensity, as well as extreme temperature pattern and associated HW, may be quite weaker than in a dry phase.

So far the research on heat and cold waves is concerned, most of them focused on the identification of HW and CW events of some specific years, and trends (Mahdi and Dhekale, 2016; Chakraborty et al., 2019; Das et al., 2020; Singh et al., 2021; Kumar et al., 2022), their mechanisms of formation (Ratnam et al., 2016) and fatalities (Malik et al., 2020). All these works reported that the north western and central parts of India are experienced heat wave-prone areas and Jammu & Kashmir as well as north western parts and some portions of Central India are cold waves prone areas in their respective period of study. However, it is noticeable from their works that heat wave occurrences over space are irregular over time-space. Long-term consistency of HW/CW occurrences of each grid can provide a reasonable view of HW/CW susceptible areas. The present study tried to identify HW and CW

consistency, frequency, and intensity gradient over space to figure out the areas with consistent or inconsistent heat/cold wave susceptibility. The study also aimed to identify the areas affected by both the extreme weather events and their nature of consistency and intensity gradient over space. Moreover, the present study also identified heat wave intensity zone using an innovative approach to be described in the method section. One area may be affected by such extreme events irregularly one or two times within a period does not always mean the area is ecologically and economically prone to such extremities. However, if a place regularly experiences these, the area may be treated as consistent HW/CW potential. Moreover, a place that experiences both the weather extremities in a consistent manner can pose immense ecological and economic stress. In this context, the consistency and intensity of both the weather extremes were planned to explore. In this context, the output of this analysis would be very vital to the policymakers to develop capacity building in different HW/CW intensity zones.

Table 1 depicts some related works of literature on extreme temperature changes, the trend of HW and CW, and associated impacts. Methods of study are also depicted in Table 1. Most of the studies done so far regarding the trend of extreme temperature change and its effect are based on percentile-based indices (Rohini et al., 2016), trend analysis using Mann–Kendall test and Sen's slope estimator (Subash et al., 2013; Pingale et al., 2014), HW/CW vulnerability index (Rohini et al., 2016, Azhar et al., 2017) in some selected period. In Indian cases, most of the studies taken Indian Meteorological Department (IMD) defined extreme temperature thresholds for analyzing HW and CW. The present study followed a unique approach to HW and CW analysis. HW/CW presence frequency approach was adopted to compute the consistency of HW/CW occurrences for every gridded data provided by IMD. Consistency means the regular appearance of an event over a while and it does signify high susceptibility to risk. The frequency of such HW/CW means the number per specific time unit. High frequency does signify high risk. A region with high HW/CW consistency and frequency does mean high intensity. The high intensity would be a good indicator for understanding HW/CW-induced potential risk. The present work computed HW/CW consistency, frequency, and intensity at a spatial scale. Moreover, the attempt of mapping the potential risk gradient of both HW and CW integrated is also novel in this work.

Table 1: Literature Review on Extreme temperature, Heat wave, and Cold wave

Literatures	Objectives	Study	Method	Findings

		area		
Rohini et al. (2016)	Measuring the trend of the heat wave	India	Excess heat wave index and Excess heat stress and factors were computed concerning 95^{th} and 90^{th} percentiles based on IMD gridded data.	In India, central and north western parts experienced expanding Heat wave frequency, total and maximum duration.
Panda et al. (2017)	Analyzes the patterns and fluctuation in the count, duration, and intensity of hot waves during 1951–2013, 1981–2013, and 1998–2013. On the other hand, this study analyzes the relation between hydro-climatic parameters and heat waves.	India	Portraying heat waves given the percentile of mean, minimum, and most extreme temperatures.	Results show that the number, recurrence, and span of daytime hot waves extended widely during the post-1980 hot and dry period over an enormous region.
Subash et al. (2013)	This study breaks down the patterns and changeability in extreme temperature indices and their effect on rice-wheat efficiency.	Two districts of Bihar state (India), the central part of the Indo-Gangetic	Mann–Kendall test (Non-Parametric) was utilized for the recognition of patterns and Sen's slope was employed to measure the extent of such patterns.	A profoundly critical positive relationship was seen between the cool days during September with rice efficiency; a negative connection was seen between wheat efficiency and the

		basin.		most extreme worth of maximum temperature (TMax) during February month.
Rajkumar et al. (2021)	This study examined the development of heat waves and warm nights over the seven agro-climatic zones.	Tamil Nadu state (India), from 1951 to 2016	Heat Wave Magnitude Index daily to concentrate on the warm spells in the daytime and nighttime temperature; Drought examination depended on the Standardized Precipitation Evapotranspiration Index.	Significant expansion in the heat wave counts, intensity, and span of the intensity and hot night episodes across Tamil Nadu between the periods 1951-1983 and 1984-2016.
Pingale et al. (2014)	Pattern examination of the average and extreme annual daily rainfall and temperature was inspected.	33 urban centers of the arid and semi-arid state of Rajasthan, India.	Statistical trend analysis technique, Mann-Kendall test, and Sen's slope estimator were used to examine trends from 1971 to 2005	The minimum, average and maximum temperature showed significant increasing warming trends on an annual and seasonal scale in most of the urban centers in Rajasthan State.
Sonali and Kumar (2013)	This study performs the spatial and temporal trend analysis of yearly, monthly	India	Non-parametric methods were used for trend detection which considers the effect of serial correlation.	A substantial change in minimum temperature during 1970–2003 over India; Significant temporal changes in

	and seasonal maximum and minimum temperatures.			temperature are found over the North Central region of India.
Malik et al. (2020)	Exploring the Spatio-temporal pattern of cold wave fatalities	India	Frequency analysis of cold wave about cold wave temperature threshold as defined by IMD	Revealed that a total of 8520 people died caused by 606 cold wave incidents with an average of 230/year mainly during December and January over northern states.
Mahdi and Dhekale (2016)	This paper is to analyze the trends and variability in extreme temperature indices from 1969 to 2013	Two important agro-climatic zones (South Bihar Alluvial zone IIIA and B) of India	The frequency and duration of heat/cold wave was determined based on the temperature thresholds as defined by IMD	Results show that in 45 years, zone-IIIA and B have encountered 251/182 and 337/140 average number of heat and cold events separately.
Azhar et al. (2017)	Assessing heat wave vulnerability including socio-economic parameters	India	Principle component approach (PCA) for computing heat wave vulnerability index (HVI)	Of the total 640 districts, the analysis identified 10 and 97 districts mainly in Central India is prone to very high and high-risk categories
Kumar et	Heat wave and	India	To understand the	Heat wave frequency

al. (2022)	heat stress patterns in four major metropolitan cities (Delhi, Mumbai, Kolkata, and Chennai) of India using 30 years of data from 1990 to 2019 during the summer season		episode of a heat wave, we have used the 95th percentile method. Furthermore, we have also used Humidity Index (HD) to evaluate the degree of discomfort and the Universal Thermal Climate Index (UTCI) to categorize the level of heat stress.	is 26-63% greater in Delhi region than in other metropolitan cities, however risks of extreme heat stress and dangerous-heat stroke events are more in the Chennai metropolitan region than remain three metropolitan regions.
Mishra et al. (2017)	This study explores population exposure to severe heat waves.	India	This study considered a variable Tmax threshold compared to the absolute values of Tmax used by the IMD, and considered both magnitude and duration of heat wave followed by Russo et al. (2015)	The global mean temperature is limited to 2.0 °C above pre-industrial conditions, and the frequency of severe heatwaves will rise by 30 times the current climate by the end-21st century
Kumar and Singh (2021)	This study estimates the number of deaths associated with exposure to heat in the different states of India	India	Descriptive statistics were applied correlating heat wave frequency and death from a socio-demographic perspective	Heat stroke-related deaths increase over time; mortality in this respect is socio-economic and demographic states respective.

153

154

Study area

India covers 3,287,263 km^2 of geographical areas with high physiographic and climatic diversity. Physiographically, three divisions are very prominent i.e. coastal plain, flood plain areas, and mountainous areas. Figure 1 can help to understand these areas with topographic variations. Sub tropical monsoon climate predominates over the region with high seasonal variation of hot and cold spells and wet and dry spells. The total annual average rainfall of India is 117cm out of which 80% is observed during the Monsoon period (Praveen et al., 2020). The annual average temperature ranges from -2 to 40°C with very high differences in extreme temperatures. Among four distinct seasons (pre-monsoon, monsoon, post-monsoon, and winter) pre-monsoon season (March to May), or summer season experiences, maximum temperature, and the winter season experience minimum temperature (Guhathakurta and Rajeevan, 2008). During extreme cold and hot seasons, entire India does not witness a uniform thermal pattern due to the high diversity of topographical height, soil differences, land use characters, etc. (Revadekar et al., 2012). Physiographic conditions are particularly shown here to clarify the fact why should temperature threshold of HW and CW be different in coastal, plains, and mountain areas. Figure 1 also shows 34 meteorological sub-divisions of IMD denoted with a short name for the convenience of analysis.

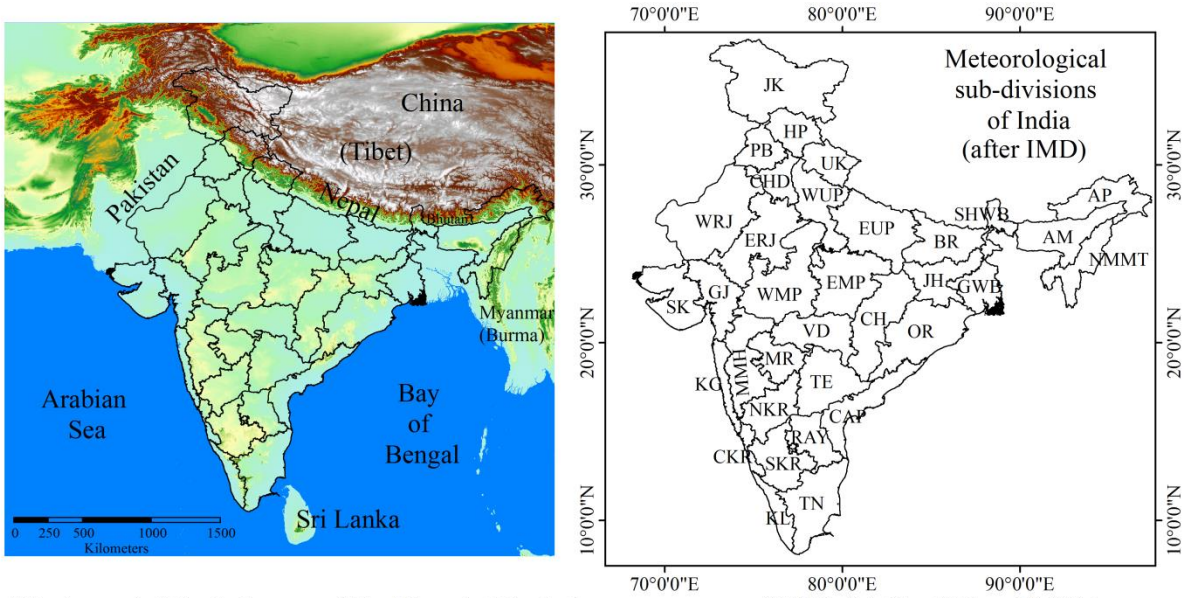

AP= Arunachal Pradesh	HP= Himachal Pradesh	SHWB= Sub-Him. W.Bengal & Sikkim
AM= Assam & Meghalaya	JH= Jharkhand	SK= Saurashtra, Kutch & Diu
BR=Bihar	JK= Jammu & Kashmir	SKR= South Interior Karnataka
CAP=Coastal Andhra Pradesh	KG= Konkan & Goa	TN= Tamilnadu & Pondicherry
CH=Chhattisgarh	KL= Kerala	TE= Telangana
CHD= Haryana. Chandigrah.& Delhi	MMH= Madhya Maharashtra	UK= Uttaranchal
CKR= Coastal Karnataka	MR= Marathwada	VD= Vidarbha
EMP= East Madhya Pradesh	NKR= North Interior Karnataka	WMP= West Madhya Pradesh
ERJ= East Rajasthan	NMMT= Naga. Mani. Mizo. & Tripura	WRJ= West Rajasthan
EUP= East Uttar Pradesh	OR= Odisha	WUP= West Uttar Pradesh
GJ= Gujarat	PB= Punjab	
GWB= Gangatic West Bengal	RAY= Rayalaseema	

Figure 1: Study area showing meteorological subdivisions after Indian Meteorological Department (IMD)

Materials

The entire analysis of extreme temperature patterns and HW and CW was done using the IMD endorsed gridded dataset available at $1^{o} \times 1^{o}$ spatial resolution. The 284 observational points over India were gridded based on Shepard's distance weighted interpolation (Srivastava et al. 2009). Extreme (Maximum and minimum) temperature data of each grid was taken from 1961 to 2020. The entire time spell was divided into two phases dry phase (1961-1990) and the wet phase (1991-2020) to show the long-term average condition of extreme events and the change between the phases. Figure 2 shows a methodological flowchart of the entire work.

Methods

Presenting seasonal distribution of extreme temperature

For showing maximum, minimum temperature distribution, 30 years, 7 years, and 1-year average maximum and minimum temperatures were computed both for phase 1 (1961-1990) and phase 2 (1991-2020). For doing this, the first 30, 7, and 1-year maximum temperature was retrieved from both the phases separately, and the average was presented in the context of the first two cases. One-day maximum data show the most extreme temperature condition within the span of phases 1 and 2 separately. In the case of minimum temperature, the same process was followed. The entire work was done at grid-level data. After getting the grid level maximum and minimum temperatures of two extreme seasons (Summer and Winter), inverse distance weighting (IDW) maps for 30 years, seven years, and one-year maximum and minimum temperature of summer and winter seasons in both the phases were done.

Analyzing Spatio-seasonal pattern of extreme temperature

The spatial distribution of temperature in different periods shows the visual impression of changing parameter characters over space and time (Dhorde et al., 2017; Feng et al., 2018). However, this analysis never helps to infer whether such change is statistically significant or not. If the pattern is found significant, then at which level it is significant? To resolve this, a hot-spot analysis of 30 years, 7 years, and 1-year extreme temperature with the aid of Getis-Ord Gi* statistic of summer and winter seasons were done. Getis-Ord Gi* is a crucial technique used for identifying statistically significant spatial high-temperature clusters (hot-spots) and low-temperature clusters (cold-spot) at different spatial scales (Ord and Getis, 1995; Wolf and McGregor, 2013). This method focuses on each grid temperature data (here) about the neighboring grid data. This analysis was done using the Hot-spot analysis tool in the Arc GIS environment. Spatial distribution maps of the extreme temperature of both phases were taken for such analysis.

The mathematical expression of computing a Hot-spot map using the said tool is depicted in Equations 1-3.

$$G_i^* = \sum_{j=1}^{n} wi,jxj - \frac{\sum_{j=1}^{n} wi,jxj - \bar{x}\sum_{j=1}^{n} wi,j}{s\sqrt{\frac{-\left[n\sum_{j=1}^{n} w_{i,j}^2 - \left(\sum_{j=1}^{n} wi,j\right)^2\right]}{n-1}}} \qquad \text{[Eq. 1]}$$

Where, Xj is the attribute value for feature j, wi,j is the spatial weight between feature i and j, n is equal to the total number of features.

$$\bar{x} = \sum_{j=1}^{n} xj \qquad \text{[Eq. 2]}$$

$$s = \sqrt{\frac{\sum_{j=1}^{n} x_j^2}{n} - (\bar{x})^2} \qquad \text{[Eq. 3]}$$

The output of extreme temperature parameters specific Gi statistic (both the phases) 284 temperature grids taken for analysis offered (a) measures of statistical significance for each grid, (b) the probability (p-value), and (c) standard deviation (z-score). Statistical significance of high or low-temperature clustering was judged using p and z values. Gi value with a p-value <0.01 and z score >2.58 indicates statistically significant maximum and minimum temperature hot-spot at 99% confidence level in different phases. Contrarily, the Gi value with a p-value <0.01 and z sore <-2.58 denotes a statistically significant temperature cold-spot at a 99% confidence level. Other levels of statistical significance of temperature were put in table 2. Differences in Gi values, their level of significance, and change in their areal extent between two selected phases can portray the nature of temperature pattern change.

Table 2: Hot and cold spot classification based on Getis-Ord Gi* approach (Tran et al., 2017; Ranagalage et al., 2018)

Gi* Hot-Spot Classes	Confidence Levels	Probability (Gi* p-value)	Standard Deviation (Gi* Z-score)
Highly Cold spot	99%	<0.01	<-2.58
Cold spot	95%	<0.05	<-1.96
Cool spot	90%	<0.10	<-1.65
Insignificant areas	Not statistically significant	0	−1.65 < z-score < 1.65
Warm-spot	90%	<0.10	>1.65
Hot-spot	95%	<0.05	>1.96
Highly hot spot	99%	<0.01	>2.58

Heat wave and Cold wave identification

According to the definition by the Indian Meteorological Department, Heat wave (HW) occurs when the temperature for consecutive two days is ≥40˚C in the plain region, ≥37˚C in the coastal region, and ≥30˚C in the Himalayan region. A cold wave occurs when the

temperature is ≤10˚C in the plain region and ≤0˚ in the mountainous region. Based on these definitions, heat and cold wave-prone areas were identified in each IMD-defined temperature grid. For doing this first, we have decomposed India into three units namely mountainous, plain and coastal plain considering meteorological units. Computation of heat wave of each zone based on IMD-defined temperature threshold limit. In the same manner, the cold wave zone was identified based on its thermal criteria (≤10˚C for plain and coastal regions, ≤0˚C for the mountainous region). Heat and cold wave-prone areas were identified for both phases 1 and 2.

Consistency of heat and cold waves

Consistency of heat and cold wave occurrences in a specific period was computed by integrating grid specific all the heat wave occurrences divided by the total number of years considered. For doing this, the first grid-based consecutive two-day temperature data was classified into two parts e.g. (1) ≥ 40˚C and (2) < 40˚C in case of a heat wave. The former class was assigned by '1' and later one was by '0' as a binary class. The number of consecutive heat wave days is a crucial factor for intensifying heat waves. Considering this, the present works counted heat waves both about (1) consecutive two-day and (2) consecutive five-day. The possible intensity is much greater than in the former case. In the same way, cold wave consistency was determined considering its threshold limit in different physiographic units as defined.

Binary classes were done for each year individually and ultimately integrated and divided by the total number of years in each phase (Eq. 4-7). The consistency value ranges from 0-1, a value near 0 means low consistency, and 1 means high or regular consistency of heat wave and cold wave appearance. For the convenience of analysis, the entire range was classified into three categories i.e. (1) highly consistent (>0.67), (2) moderately consistent (0.33-0.67), and (3) low consistent (<0.33) (Sarda and Das, 2018)

$$HWPF_2 i = \frac{\sum_{F=1}^{N} PFHW_2 i}{N_i} \qquad \text{[Eq. 4]}$$

$$CWPF_2 i = \frac{\sum_{F=1}^{N} PFCW_2 i}{N_i} \qquad \text{[Eq. 5]}$$

$$HWPF_5 i = \frac{\sum_{F=1}^{N} PFHW_5 i}{N_i} \quad \text{[Eq. 6]}$$

$$CWPF_5 i = \frac{\sum_{F=1}^{N} PFCW_5 i}{N_i} \quad \text{[Eq. 7]}$$

HWPF$_2$i= Heatwave presence frequency (consecutive two days) of the ith grid; $PFHW_2 i$ = Presence of heat wave in binary format (consecutive two days) for ith grid experiences; Ni= number of total years considered for analysis in the ith grid.

CWPF$_2$i= Cold wave presence frequency (consecutive two days) of the ith grid; Fcw$_2$i= Presence of cold wave in binary format (consecutive two days) for ith grid experiences; Ni= number of total years considered for analysis in the ith grid. Equations 6 and 7, F_5 refer to heat/cold waves for consecutive five days.

Measuring the frequency of heat and cold waves

The frequency of heat waves means the number of heat wave occurrences per unit time (here considered year). The frequency of heat waves for consecutive two-day and five-day was counted for each year and combined about phases 1 and 2 separately. In the same way, cold wave frequency was counted and expressed as a percentage of the total day count of a period (Eq. 8-11). It was assumed that high-frequency heat/cold waves and the duration of heat wave spell signify greater susceptibility.

$$HWF_2 i = \frac{\sum_{F=1}^{N} FHW_2 i}{N} \times 100 \quad \text{[Eq. 8]}$$

$$CWF_2 i = \frac{\sum_{F=1}^{N} FCW_2 i}{N} \times 100 \quad \text{[Eq. 9]}$$

$$HWF_5 i = \frac{\sum_{F=1}^{N} FHW_5 i}{N} \times 100 \quad \text{[Eq. 10]}$$

$$CWF_5 i = \frac{\sum_{F=1}^{N} FCW_5 i}{N} \times 100 \quad \text{[Eq. 11]}$$

$HWF_2 i$ = Heat wave frequency for consecutive two days in the ith grid; $FHW_2 i$ = Frequency of heat wave (consecutive two days) in the ith grid; N= total number of days in selected period; $CWF_2 i$ = Cold wave frequency for consecutive two days in the ith grid; $FCW_2 i$ = Frequency of cold wave (consecutive two days) in the ith grid. In Equations 10 and 11, HWF_5 and CWF_5 refer to heat/cold waves for consecutive five days, other symbols signify the same as denoted.

Measuring the intensity of heat and cold waves

Here heat/cold wave intensity was defined by combining consistency and frequency of occurrences. A place with high consistency and frequency does indicate the high intensity of heat/cold waves. Its socio-ecological and ecological implication is very sensitive. It was computed by multiplying the consistency and frequency of heat/cold wave of each temperature grid using equations 12-15. Consecutive two-day and five-day consistency was multiplied by respective frequency. Heat or cold wave intensity values vary from 0 to infinity, where more value indicates more intensity.

$$HWI_2 i = HWPF_2 i \times HWF_2 i \quad \text{[Eq. 12]}$$

$$HWI_5 i = HWPF_5 i \times HWF_5 i \quad \text{[Eq. 13]}$$

$$CWI_2 i = CWPF_2 i \times CWF_2 i \quad \text{[Eq. 14]}$$

$$CWI_5 i = CWPF_5 i \times CWF_5 i \quad \text{[Eq. 15]}$$

Where, $HWI_2 i$= Two days heat wave intensity of ith grid; $CWI_2 i$ = Two days cold wave intensity of ith grid

Grid-specific time series analysis of HW/CW frequency from 1961 to 2021 was represented in a heat map for different physiographic units.

Mapping co-existence of HW and CW

For mapping co-existence characters of HW and CW, 2-day and 5-day consistency and intensity maps were reclassified defining absent, high, moderate, and low classes. After that

HW and CW matrices were developed indicating different possible combinations (theoretically 16 possible classes) of co-existence. This map was prepared for 2-day, 5-day consistency, and intensity in phases 1 and 2. Co-existence of both high-intensity HW and CW is highly susceptible to the ecosystem and human health (Stillman, 2019; Weilnhammer et al., 2021; Drakes and Tate, 2022).

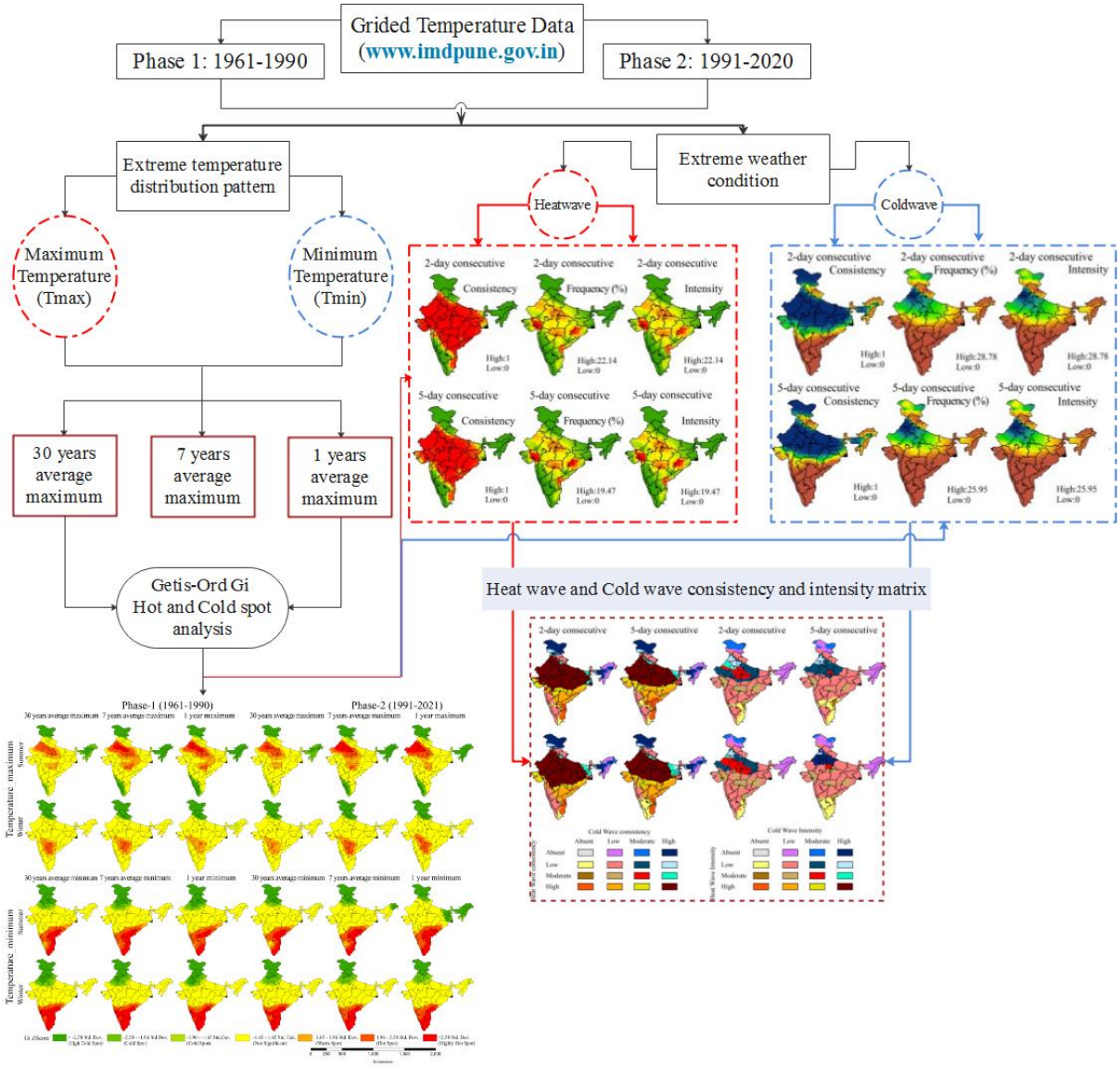

Figure 2: Methodological flow chart of the work

Results

Spatio-seasonal distribution of extreme temperature

Figure 3 depicts the phase-wise extreme temperature distribution in summer and winter months for about 30 years, 7 years, and 1-year maximum/minimum. During the summer months, entire north western India, central India, and eastern India experience high maximum

temperatures (Figure 3). The one-day maximum temperature effect is more pronounced over a wider geographical area followed by 7-year and 30-year average maximum temperature. Range of 30 years, 7 years, and 1-year maximum during summer season were respectively 20.53 to 45.26, 31 to 46.66 and 32.99 to 47.49 in phase 1 and 19.45 to 45.30, 30.93 to 46.60 and 31.80 to 48.46 in phase 2 respectively. During the winter season, 30 years, 7 years, and 1-year maximum temperature between two phases show little significant change. During the winter season, except in Jammu and Kashmir, the rest part of India showed extreme temperatures above >30˚C. Minimum extreme temperature in summer and winter seasons varies from -5.07-22.26˚C and -9.12˚C to 19.39˚C in phase 1, whereas in phase 2 -3.89-22.61 ˚C and -9.02-20.44˚C in summer and winter seasons. It is observed that the minimum extreme temperature rise in the summer and winter seasons from phase 1 (1961-1990) to phase 2 (1991-2020).

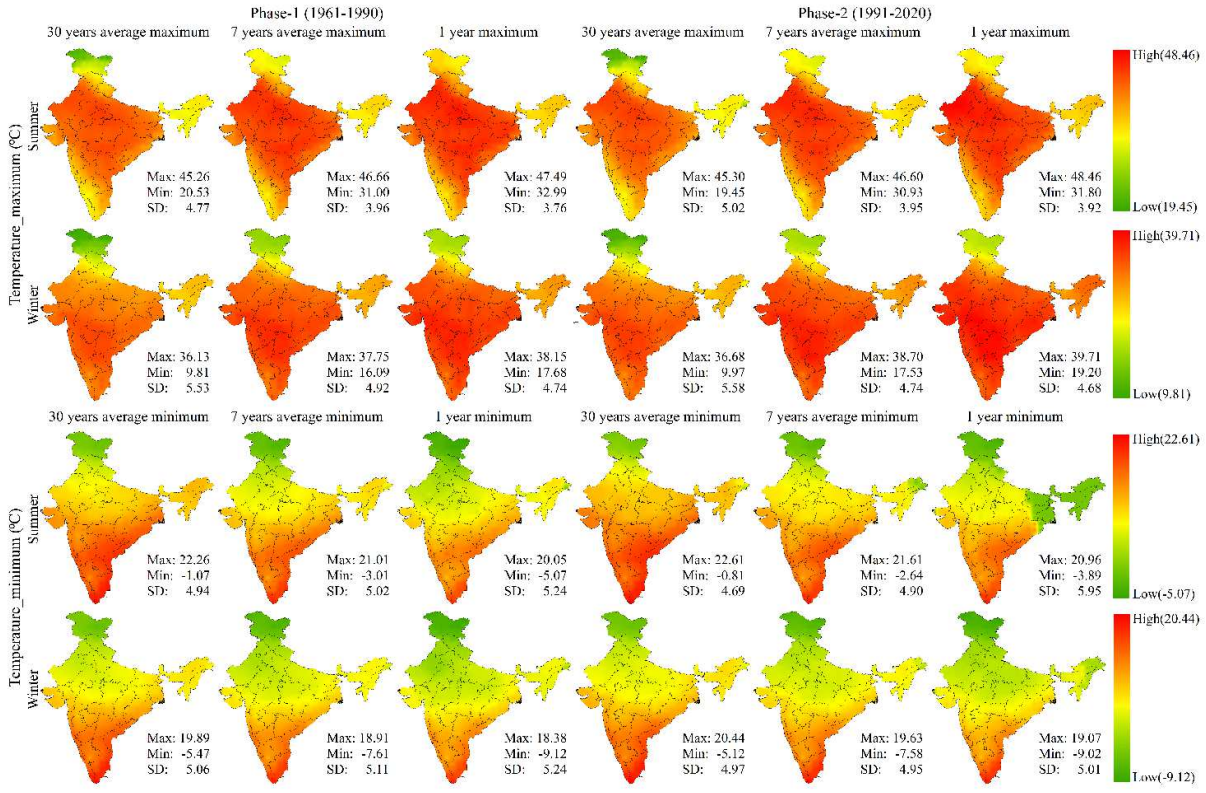

Figure 3: Spatial distribution of extreme temperature during summer and winter seasons in Phase-1 (1961-90) and Phase-2 (1991-2020)

Spatio-seasonal pattern of extreme temperature

Spatial pattern of extreme temperature's hot and cold spot for summer and winter months in both the phases is shown in figure 4. 30-year maximum temperature hot-spot of summer

season recognized major parts of 8 meteorological subdivision units as a statistically significant hot-spot (>95% confidence level) patch in phase 1. In phase 2, this area was squeezed into small patches in 6 meteorological subdivision units indicating the noticeable change in the hot-spot pattern. About 4% of the statistically significant (95% or more) area was turned into an insignificant area. Significant cold-spot (99% level) was found in J&K and north eastern India in phase 1, but it was found quite a similar result in phase 2. Statistically significant hot-spot at 99% confidence level was increased from 0.07% to 1.16% and hot-spot at 95% confidence level from 9.04% to 9.29%. About 7-year and 1-year maximum temperature, 8 and 11 metrological subdivisions were recognized as significant hot spots (95% and 99% levels) in phase 1 and the pattern was noticeably shifted towards the western direction in phase 2. 6 metrological subdivisions were identified as significant (99%) cold-spot in phase 1 and this pattern was recognized almost unchanged in phase 2 for & years and One-year average extreme temperature.

The hot-spot pattern was also analyzed about the minimum temperature of 30 years, 7 years, and 1- year. 30 years average minimum temperature in the summer season shows that a wider part of the Deccan trap region (MR, RAY, NKR, TE, and VD) falls under hot-spot (95-99%) covering 9.59-9.66% area and north India covering 2 meteorological units with an area of 3.77-14.36% fall under cold-spot (95% and 99%) in phase 1. This pattern is almost uniform for 7 years of average minimum extreme temperature cases during this phase. But the 1-year extreme temperature in the summer season shows a quite different picture. In phase 2, Along with north India, north-eastern 3 meteorological subdivisions and some parts of eastern India fall under the category of cold spot (95% confidence level). In phase 2, the spatial pattern of significant highly hot and cold-spot (99%) does not show any observable variation but the areal extent under significant hot and cold spots has been squeezed (Table 3).

The maximum temperature during the winter season about 30 years, 7 years, and 1- year average shows that J&K, HP, UK, and PB sub-divisions were recognized as significant (99%) cold-spot covering 11.53-11.97% of the area in phase 1 to 11.41-11.97% area in phase-2. No such change was identified in phase 2. About 30 years, 7 years, and 1 year in hot-spot, 0.59-4.64% areas of central Deccan plateau physiographic units under 10 meteorological sub-divisions were found as statistically significant hot-spot at a 95% confidence level in phase 1. No area was found significant at the 99% level. In the case of 1-year maximum, areal extent was proliferated by 0.59 to 6.09%, while in the case 30 years average, noticeable decline in areal extent (Table 3)

About winter minimum in phase 1, 13.70-15.05% area at 99% and 4.52-5.58% area at 95% levels were found significant cold-spot covering 2 meteorological sub-divisions. Conversely, about 20% areas come under significant (95-99%) hot-spot (Table 3) covering 12 meteorological sub-divisions. The conditions are almost uniform in 30 years, 7 years, and 1-year average minimum.

From the analysis, it is very evident that there is no major shift in the extreme event distribution pattern with statistical significance between phases 1 to 2. However, the 1-year hot and cold-spot pattern of maximum and minimum temperatures is more pronounced than average extremes indicating increasing uncertainty of this occurrence. Therefore, 30 years and 7 years of average study is a very fruitful approach for examining extreme temperature situations.

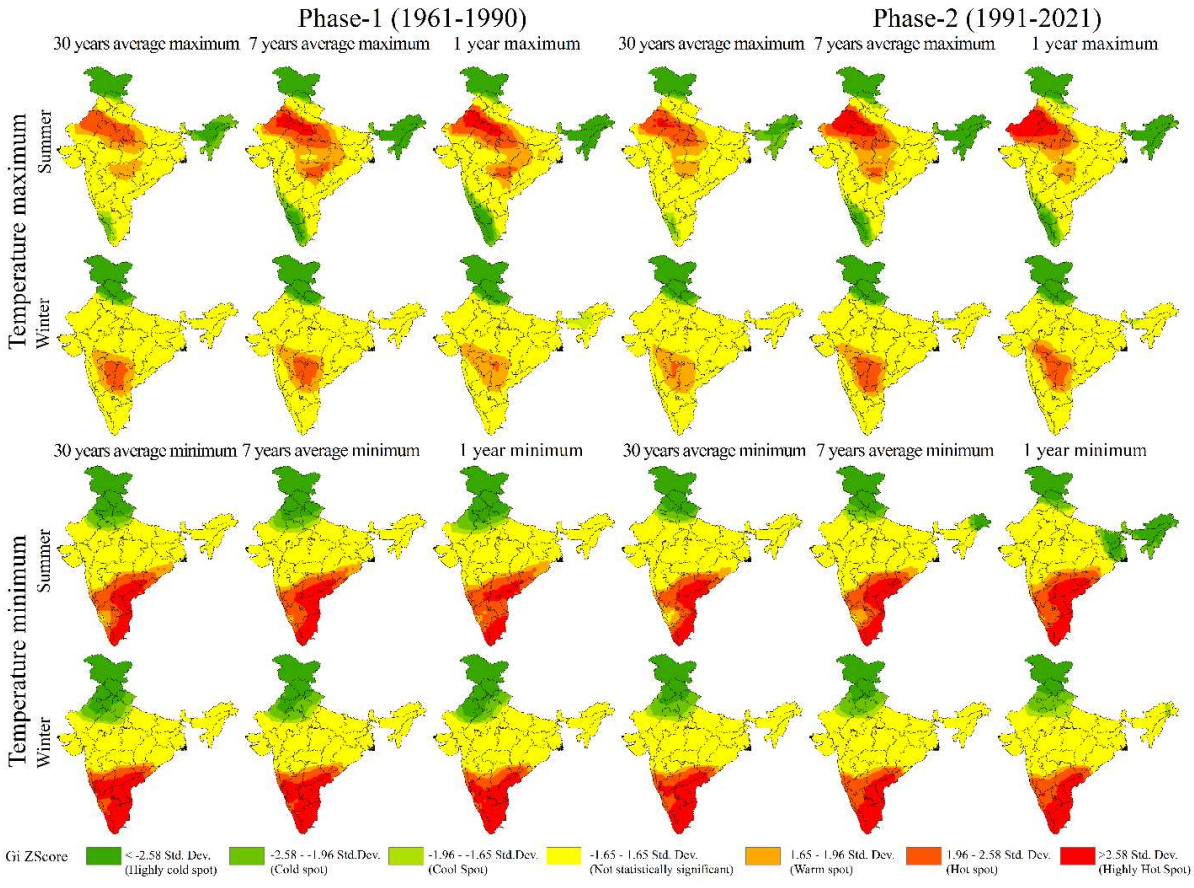

Figure 4: Hot and cold spots of maximum and minimum temperature during summer and winter seasons of Phase-1 (1961-90) and Phase-2 (1991-2020)

Table 3: Hot spot and cold spot of extreme temperature in summer and winter seasons of phases 1 and 2

Season	Extreme temperature category	Gi* Hot-Spot Classes (Z-score)	1-year		7-year		30-year	
			Phase-1	Phase-2	Phase-1	Phase-2	Phase-1	Phase-2
Summer	Maximum Temperature	Highly Cold spot (<-2.58)	19.46	18.18	18.72	18.48	11.66	10.61
		Cold spot (-2.58--1.96)	3.69	4.08	3.43	3.62	6.22	6.17
		Cool spot (-1.96--1.65)	1.83	2.24	1.99	1.88	2.36	2.79
		Not statistially significant	47.69	51.69	46.48	48.97	59.60	59.25
		Warm spot (1.65-1.96)	12.59	8.82	13.62	11.89	11.05	10.73
		Hot spot (1.96-2.58)	10.20	7.26	11.79	8.64	9.04	9.29
		Highly Hot spot (>2.58)	4.55	7.73	3.97	6.53	0.07	1.16
Winter	Maximum Temperature	Highly Cold spot (<-2.58)	11.97	11.97	11.94	11.95	11.53	11.41
		Cold spot (-2.58--1.96)	0.97	1.15	1.07	1.04	1.32	1.38
		Cool spot (-1.96--1.65)	2.82	0.95	0.57	1.00	0.58	0.59
		Not statistially significant	72.35	72.72	73.34	72.20	73.98	75.02
		Warm spot (1.65-1.96)	11.30	7.12	8.45	7.68	7.97	10.60
		Hot spot (1.96-2.58)	0.59	6.09	4.64	6.13	4.62	1.00
		Highly Hot spot (>2.58)	0	0	0	0	0	0
Summer	Minimum Temperature	Highly Cold spot (<-2.58)	15.18	18.19	14.56	13.41	14.36	12.59
		Cold spot (-2.58--1.96)	4.06	6.41	4.06	3.30	3.77	2.56
		Cool spot (-1.96--1.65)	2.56	1.48	2.38	2.05	1.91	1.84
		Not statistially significant	53.06	48.17	54.39	57.85	55.49	60.67
		Warm spot (1.65-1.96)	4.73	3.67	4.11	4.35	5.23	4.93
		Hot spot (1.96-2.58)	12.74	9.58	9.71	8.50	9.59	8.19
		Highly Hot spot (>2.58)	7.68	12.49	10.79	10.54	9.66	9.22
Winter	Minimum Temperature	Highly Cold spot (<-2.58)	15.05	10.46	13.70	11.52	14.87	12.43
		Cold spot (-2.58--1.96)	4.52	5.65	5.58	5.84	5.55	5.91
		Cool spot (-1.96--1.65)	2.07	4.12	2.67	2.49	2.43	2.73
		Not statistially significant	57.19	59.72	56.43	60.22	54.92	57.89
		Warm spot (1.65-1.96)	2.54	2.19	2.33	1.91	2.27	1.95

		Hot spot (1.96-2.58)	5.76	7.61	5.27	7.55	5.67	6.36
		Highly Hot spot (>2.58)	12.88	10.26	14.02	10.46	14.28	12.72

Consistency, frequency, and intensity of heat and cold waves

Heat wave (HW) characters

Figure 5 depicts consecutive 2-day and 5-day heat wave consistency, frequency, and intensity of HW in phases 1 and 2. About 2-day consistency, about 65% of the area (Table 4) over Northwestern, Central, and Eastern India (19 meteorological sub-divisions) was found highly consistent (>67%) in heat-wave appearance in both the phases without having any significant difference. The frequency of heat-wave (in case of 2-day consecutive) varies from 0-22% of total days in both the phases. 5-day consecutive heat wave frequency patches covering around 85% area to the total area were identified around eastern Gujrat, Delhi, Chhattisgarh, north western Odisha, and Telangana regions. The average annual frequency in the Gujrat region was 62 per year in phase 1 and 70 per year in phase 2. In the Delhi region, it was 36 and 38/year in phases 1 and 2 respectively. The intensity pattern of HW is almost with some minor spatial-temporal changes. The areal extent of HW consistency, frequency, intensity domain, and their spatial pattern is slightly less in the case of consecutive 5-day HW analysis. Such spatial juxtaposition explains the fact that most of the regions experience consecutive two-day HW often last 5-day or more. If year-wise of short-term variation is examined one can get higher regional variation, however, long-term average database analysis quite eliminated the extremities to some extent.

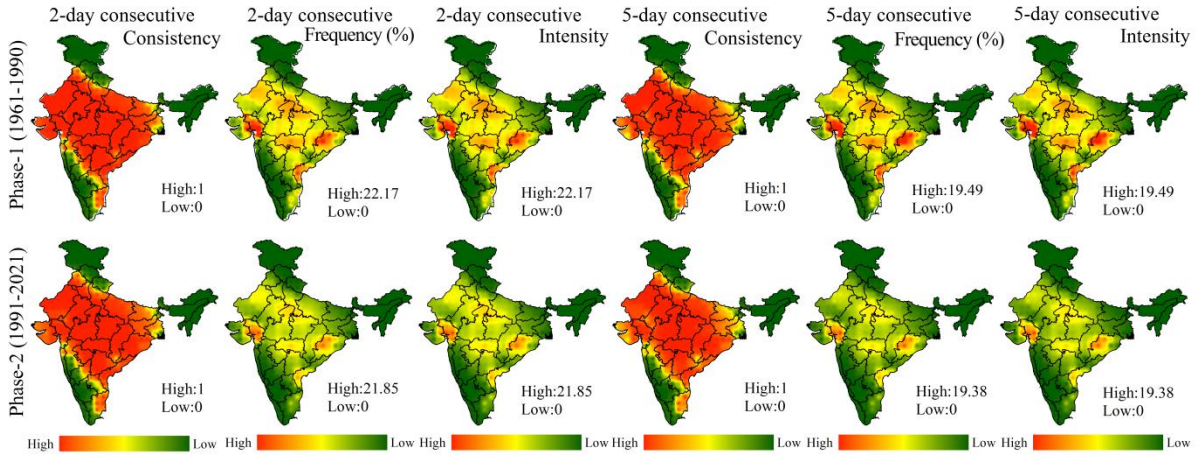

Figure 5: Consecutive 2-day, 5-day Heat wave consistency, frequency, and intensity in Phase-1 (1961-90) and Phase-2 (1991-2020)

Cold wave (CW) characters

Figure 6 shows the CW consistency, frequency, and intensity in phases 1 and 2. Consecutive 2-day CW consistency covers J & K and north-western India, and a wider part of the Gangetic plains, Central India, and parts of the Northeastern hilly region in phase 1. In phase 2, it was intensified in the north-eastern hilly region, and wider part of West Bengal while declining to some extent in the Saurashtra region (Figure 6). The geographical location of a consecutive 5-day CW surge area is almost similar to a 2-day CW surge, however, the major CW tract over north-western, central India was found squeezed from its southern fringe. About 49 to 58% area was found where there was a co-existence of consistent (67 % or above) 2-day and 5-day CW. In phase 2, about 1 % area of the high consistent area was proliferated. Some patches were found where high consistency was increased. The frequency and intensity of CW were found very high (>20%) in the northern extreme of J & K and relatively high (10-20%) in north-western India in phase 1. While the areal extent of the frequency and intensity of CW declined from phase 1 to phase 2. For 2-day consecutive 5.82% area falls under high cold wave frequency and intensity in phase 1, whereas in phase 2 this category covers 2.25% of the total mainland. Regional disparity in the change of CW is very prominent in this analysis. If the analysis is done considering the entire India shift of high CW intensity zone to relatively lower zones (Table 4) and extension of low to moderate intensity areas were recorded.

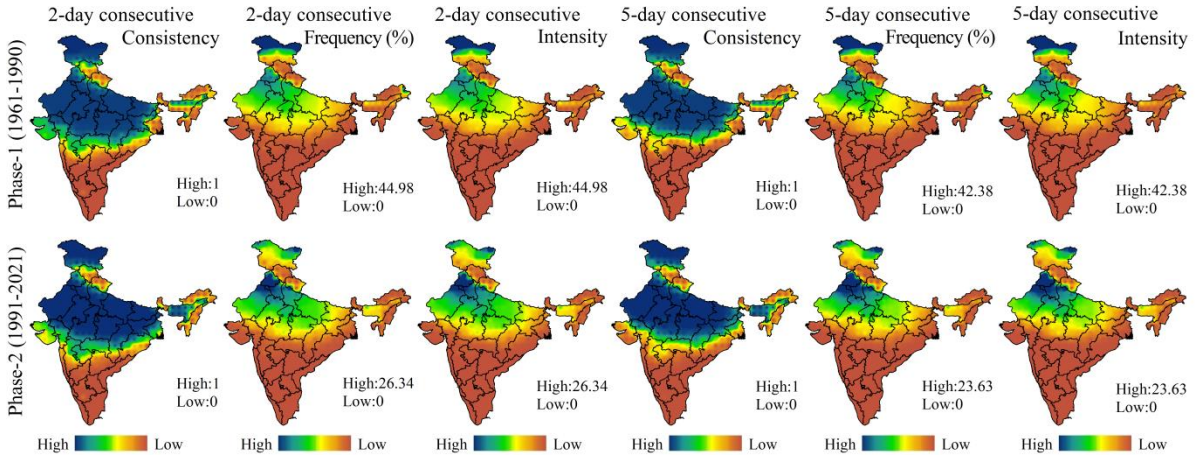

Figure 6: Consecutive 2-day, 5-day Cold wave consistency, frequency, and intensity in Phase-1 (1961-90) and Phase-2 (1991-2020)

Table 4: Percentage (%) of area for Heat and cold waves in Phase-1 and Phase-2

Criteria	Heat wave			Cold wave	
	Consistency class	Phase-1	Phase-2	Phase-1	Phase-2
2-day consecutive	Absent	14.35	14.38	6.19	4.14
	<0.33	14.63	14.69	24.14	25.96
	0.33-0.67	4.79	6.01	11.94	11.59
	>0.67	66.22	64.92	57.74	58.31
5-day consecutive	Absent	14.80	14.80	9.71	11.01
	<0.33	15.55	16.36	28.44	27.78
	0.33-0.67	6.91	8.17	11.98	11.01
	>0.67	62.74	60.67	49.87	50.19
2-day consecutive	Frequency class	Phase-1	Phase-2	Phase-1	Phase-2
	Nil	14.35	14.38	6.19	4.14
	<10%	64.27	57.71	60.51	67.82
	10--20	21.26	27.66	27.49	25.79
	>20	0.11	0.26	5.82	2.25
5-day consecutive	Nil	14.80	14.80	9.714	11.01
	<10%	77.76	73.15	68.999	76.03
	10--20	7.44	12.01	19.076	12.44
	>20	0	0.03	2.211	0.52
2-day consecutive	Intensity class	Phase-1	Phase-2	Phase-1	Phase-2
	Absent	14.35	14.38	6.19	4.14
	<10%	64.35	57.90	60.54	67.84
	10--20	21.18	27.47	27.46	25.77
	>20	0.11	0.25	5.82	2.25
5-days consecutive	Absent	14.80	14.80	9.71	11.01
	<10%	77.84	73.30	69.02	76.03
	10--20	7.36	11.87	19.06	12.44
	>20	0	0.03	2.21	0.52

Grid-specific trend of HW and CW frequency

Although long-term average HW frequency does not show any significant difference between phases 1 and 2, however, grid-specific yearly HW frequency of coastal and plain regions presented in heat maps (Figure 7) reflects that over the progress of time HW frequency was observed to increase particularly in between 2010-2020. The coastal region grid id 0 to 52 (Supplementary Figure S1) shows consistently high-frequency HW. In the plain region, this

trend is clearer (Figure 7). Five days frequency is 5-7% lesser than the two-day frequency. HW frequency was found significantly high in the five high-intensity HW patches as indicated earlier. A large number of grids are found where there is no definite trend of change of HW except in the high-intensity patches and surroundings. In the coastal region, HW frequency is quite greater than in the plains region. The mountainous region did not register any HW so far as the present study length is concerned. The grid-specific trend of CW frequency showed that a good many grids in J & K and adjoining parts recorded a gradual decline of its frequency while some grids of north-western and central India recorded an increasing trend of CW frequency. Heat maps of CW frequency were put here separately for coastal and plain zones respectively (Figure 8).

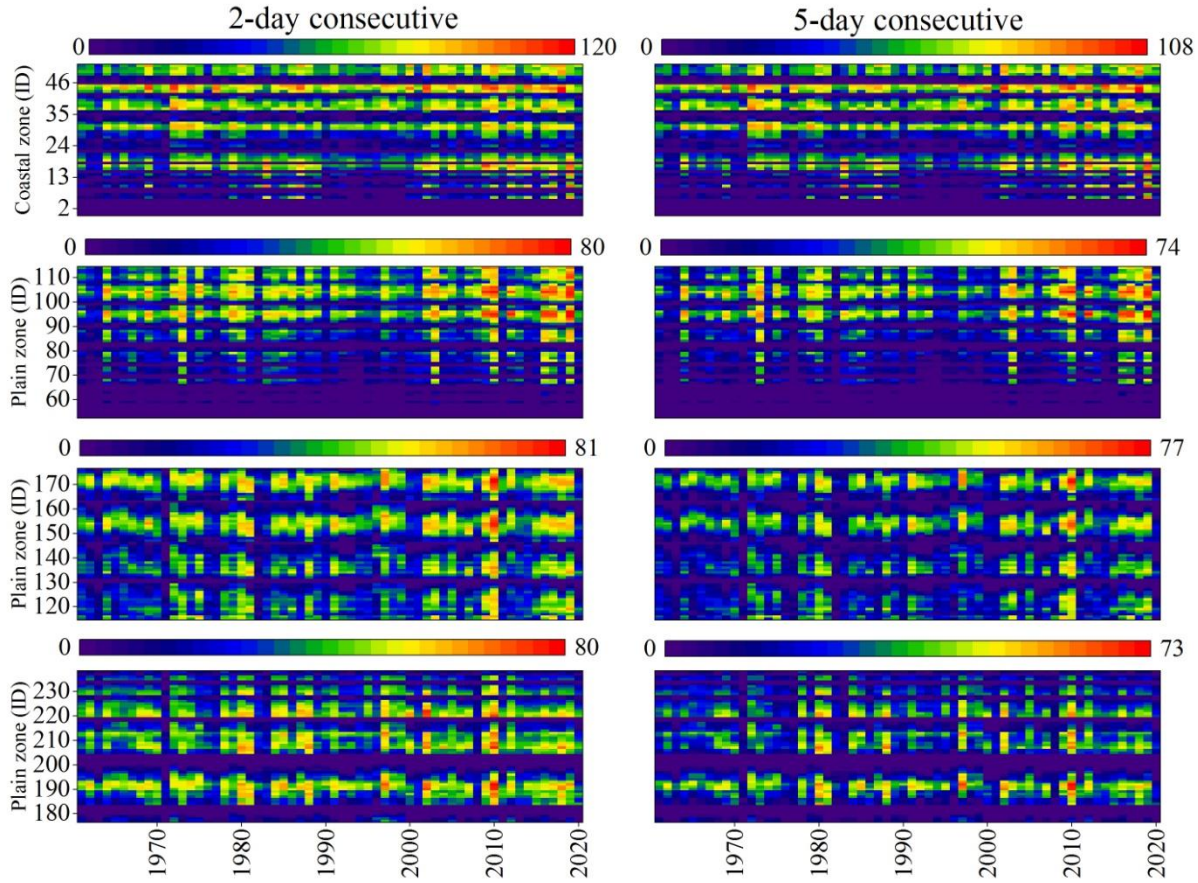

Figure 7: Grid-specific yearly 2-day and 5-day consecutive heat wave frequency in coastal and plain zones from 1961 to 2020

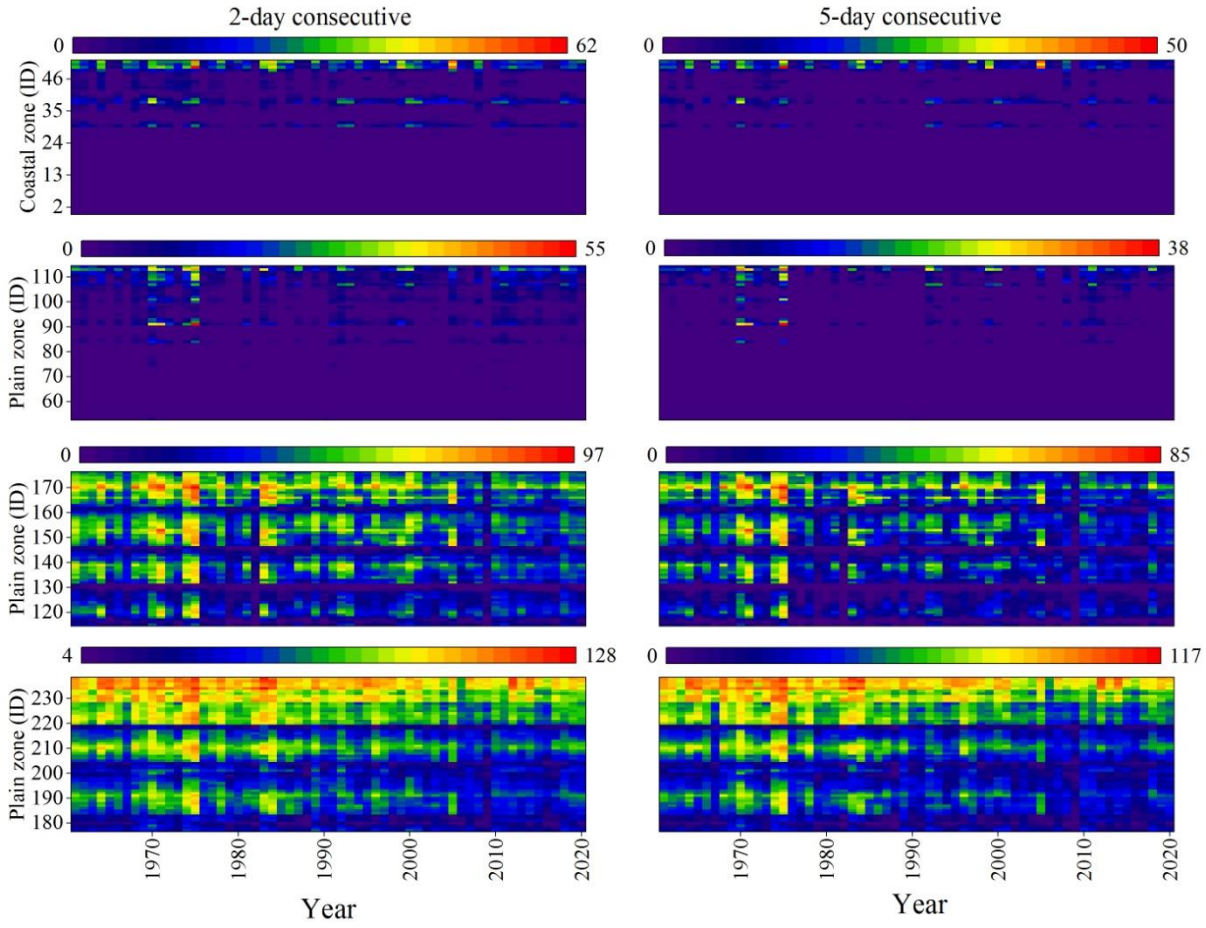

449

450 **Figure 8:** Grid-specific yearly 2-day and 5-day consecutive cold wave frequency in coastal
451 and plain zones from 1961 to 2020

452 **Dual hazard (HW and CW) matrix**

453 Figure 9 depicts the co-existence character of HW and CW in the consistency and intensity.
454 HW and CW matrices were generated both about consecutive two and five-day consistency
455 and intensity. About 45.53% of the area over Northwestern and Central India is characterized
456 by both highly consistent (consistency level: >0.67) HW and CW. The areal extent of five
457 consecutive days of high HW and CW consistency is found in 35.93% of areas, which is
458 lesser than two days. Regarding HW and CW intensity matrix, two patches in the Rajasthan
459 and Delhi regions covering an area of about 11.26% area of the total area were identified
460 where the co-existence of both high HW and CW is noted. Phase-wise changes in location
461 and the areal extent of high consistency and intensity of HW and CW are not significantly
462 observed. While moderate-intensity HW and high-intensity CW areas were identified in parts
463 of Rajasthan, Punjab, and Haryana in phase 1 were reduced to some extent in phase 2.

464

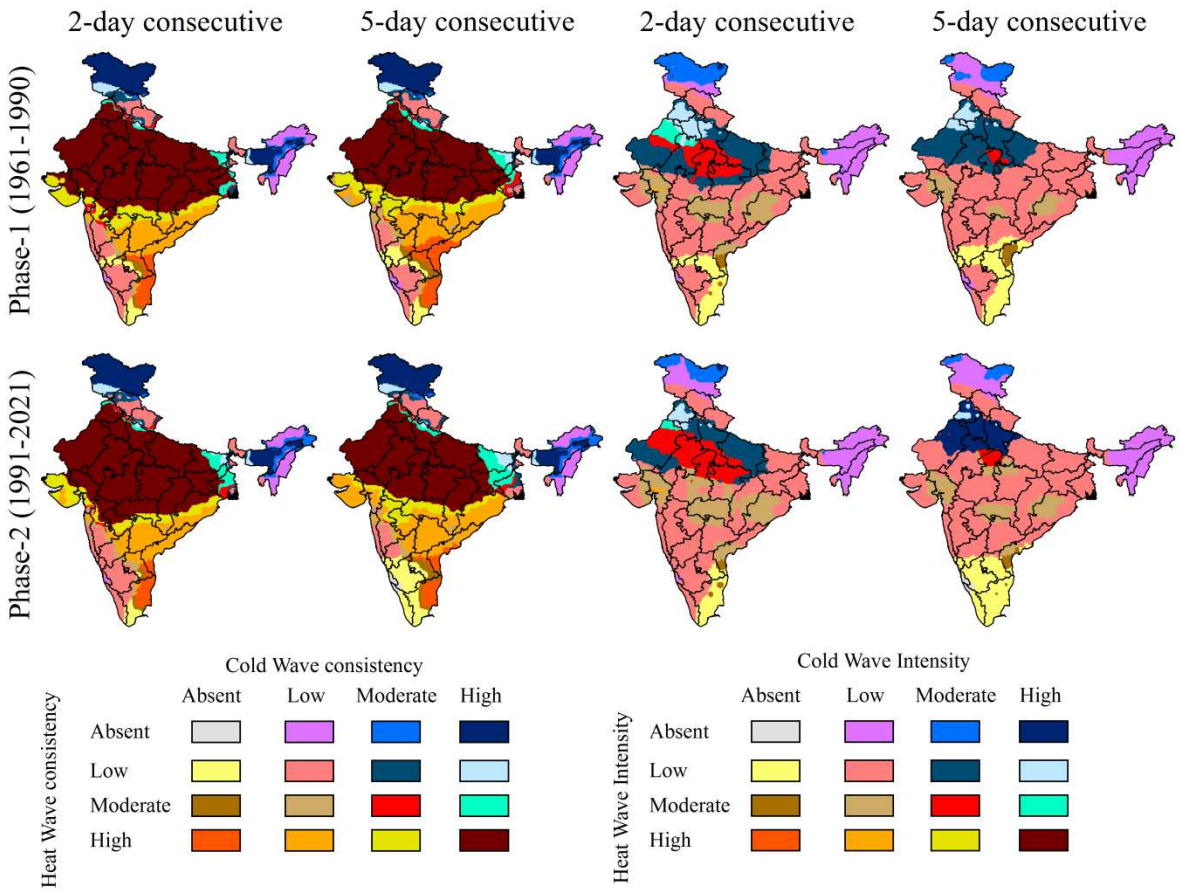

Figure 9: Consecutive 2-day and 5-day HW and CW consistency and intensity matrix in Phase 1 and Phase 2

Discussion

Spatial pattern analysis revealed that north western and central India was recognized as statistically significant hot-spot about maximum summer temperature and northern and north-western India was recognized as significant cold-spot in both the phases with some changes in areal extent and intensity. Comparison of hot and cold-spot areas coincide with HW and CW maps prepared based on two and five consecutive days of extreme temperature (1-year, 7 years, and 30 years). So, the hot and cold-spot analysis would be an alternative for finding out HW and CW potential areas.

Historical records show that HW mainly occurred during summer months like March, April, May, and June mainly in the continental climate dominated by a subtropical monsoon climate. Wide parts of the Indian mainland experience HW during the summer months but its occurrences, frequency, and intensity are not consistent enough. But parts of North West and Central India are highly susceptible to HW. However irregularity, and regularity of HW are

linked with both regional and global climatic regimes like the presence of anomalous anti-cyclonic flow over northern India, quasi-stationary Rossby wave, major climatic anomalies such as Pacific Decadal Oscillation (PDO), El Nino/Southern Oscillation (ENSO), North Atlantic Oscillation (NAO), etc. (Rohini et al., 2016; Naveena et al., 2021; Dar and Dar, 2022). Variability of the CW phenomenon is also associated with some regional and global climate anomalies (Serrano-Notivoli et al., 2022; Parliari et al., 2022)

The presence of positive height anomalies and the presence of anomalous anticyclonic conditions over northern tracts of India at the levels of 500 hPa and 200 hPa promote consistent heat wave occurrences across this region (Rohini et al., 2016). Anomalous cyclonic and anticyclonic flow in the mid-latitude of the Northern hemisphere in pursuance of the presence of the Rossby wave pattern is one of the major reasons behind heat waves over this region. The presence of the anomalous high and low-pressure cells over the North Atlantic and adjacent Europe and an anomalous low over central Asia respectively insists anticyclonic condition over northern India where HW predominates (Rohini et al., 2016). Perkins (2015) reported that anti-cyclonic blocking also caused major HW over Russia and Europe. Such blocking triggered by anti-cyclone does not permit assimilation of warm tropical and cold polar air and promotes surface warming. In the case of India, the effect of sub-tropical high or persistent high (Perkins, 2015) and accompanying anti-cyclonic flow at the upper and middle troposphere enforce sinking motion and this condition leads to warming surface caused by adiabatic shrinkages (Rohini et al., 2016). This condition again is responsible for the continuous soil moisture depletion and reduction of the atmospheric water (Lorenz et al., 2010). Moreover, summer solstice and positive diurnal heat balances for long days are also responsible for the nucleation of HW in north-western and central India. In the northwestern part of India, the presence of Thor desert, very least moisture availability, and long photo hours make the situation grave. Antecedent moisture availability may be a crucial determinant of the variability of HW incidents. For example, the year with high antecedent moisture may have less likelihood of HW.

Apart from this, global climate anomalies in the central Pacific and the tropical Indian Ocean are also linked with such HW. Kenyon and Hegerl (2008) and Arblaster and Alexander (2012) reported the effects of North Atlantic Oscillation (NAO), El Nino/Southern Oscillation, and Pacific decadal oscillation (PDQ) on the variation of HW frequency and intensity. Warming of the tropical Indian Ocean surface concerning ENSO increases the HW occurrences (Rohini et al., 2016; Naveena et al., 2021). One degree rise in sea surface

514 temperature can promote temperature rise across a wider part of India (Revadekar et al.,
515 2009; Panda et al., 2014). Murari et al. (2016), Rohini et al. (2016), and WMO (2022) also
516 reported increasing the likelihood of ENSO can enhance the frequency and intensity of HW
517 in the Indian subcontinent. In the present study, HW and CW frequency represents through
518 heat maps in Figures 7 and 8. This result is quite accordant with the result of Revadekar et al.
519 (2009), Panda et al. (2014), Panda et al. (2017), and Dubey and Kumar (2022). Long days
520 average did not show any prominent increase of HW frequency and intensity over a wider
521 part of HW susceptible areas but a good many grids in this tract were found where such trend
522 is clear. The regional character of high temperature and HW occurrences are linked with land
523 use characters (Habeeb et al., 2015; Findell et al., 2017; Pal and Ziaul, 2017). High-intensity
524 HW patches over Delhi mega cities and its surrounding proves that the urban landscape
525 insists on HW intensity. Densely built areas and the poor presence of green and blue spaces
526 are responsible for this enhanced HW condition in association with climatic events.

527 Extreme northern India, Northwestern India was found highly susceptible to both consecutive
528 2-day and 5-day CW occurrences. High altitude and decrease of temperature as per normal
529 and adiabatic lapse rate, expansion of airmass in high altitude is the main cause behind CW
530 occurrences in J & K and its adjoining areas. The spatial extent of CW susceptibility and its
531 intensity was found maximum during the winter season due to the winter solstice caused by
532 the southern migration of sun and oblique sun rays in the Northern part of India, particularly
533 in this part located in relatively higher northern latitude (Sanjay et al., 2020). Now, why CW
534 consistency and intensity was found high in north-western and central India particularly
535 Rajasthan, Delhi, and adjoining parts? Due to the winter solstice in the northern hemisphere,
536 usually northern India receives oblique sunrays with around 10 hours of photo duration, but
537 the return time is more. It causes a lowering of temperature in this area (Miller, 2019). The
538 location of Thor desert in Rajasthan and adjoining parts where reflectivity is greater than
539 Gangetic plain is one of the major causes behind it. Another major issue of CW is needed to
540 be explained. Previous studies on the mechanism and maintenance of CW in the Indian sub-
541 continent showed that intrusion of cold air train from the Ural-Siberia region (500 hPa eddy
542 stream function positive anomalies) through anomalous trough over South China is the most
543 crucial factor for regular CW occurrences (Bedekar et al., 1974, Ratnam et al., 2016). Its
544 intensity and interruption are highly associated with CW frequency and its severity in north
545 and north-western India. Western disturbances (WD) often insist on the formation and
546 intensification of CW in north and north-western India (Bedekar et al., 1974). WD is a good

tract eastward-moving westerlies troughs in the upper tropospheric north of 20°N energized by the subtropical westerly jet stream and often found extending up to the lower troposphere (Rao & Srinivasan, 1969; Bedekar et al., 1974; Ratnam et al., 2016). It is also responsible for transporting cold air from the higher latitude and intruding CW into India. Prevailing duration, break-in WD often determines the behavior of CW in India particularly in the northern halves of India. Bedekar et al. (1974) also explained CW variability in the low-pressure system in the northern part of the Arabian sea. A low-pressure system enhances the inflow of cold wind from higher latitudes and consequently a cold environment over northern India. Akhila et al. (2022) also reported that sea surface temperature anomaly triggered cyclonic events in the Arabian sea waking up the insurgence of CW. The present study also exhibited that the frequency and intensity of CW were increased by 13-26% in the northwestern CW tract and it was found to extend eastward over time. Frequency enhancement over time was also according reported by Panda et al. (2017), and Malik et al. (2020). It clarified the fact that anomalies of some global climatic events are also linked with CW incidents and their variability (Ratnam et al., 2016).

Ratnam et al. (2016) establish a link between El Nino and La Nina phenomena over the Pacific ocean. They correlated occurrences of Type 1 CW (cooler temperature effects across most parts of India) with La Nina and Type 2 CW (mainly in northwest India) with El Nino events. Mukhopadhyaya et al. (2021) established that prolonged La Nina is linked with high-intensity CW in India. Akhila et al. (2022) also reported the signature of tropical cyclone-induced wakes of CW in India. So arrhythmic pattern of such global climatic events is largely responsible for the spatial and temporal variability of CW incidents. Cai et al. (2021) reported that ENSO sea surface temperature variability and extreme ENSO incidents are likely to be increased amid the global warming scenario. It may further increase the intensity and variability of CW in the Indian sub-continent.

The present study incorporated all the gridded data of India and showed long-term extreme average temperature for 30 years, 7 years, and 1-year conditions pattern with consequent HW and CW pattern in India from 1961 to 2020. 30 years average extremities were presented and compared since 1961-1990 was defined as dry phase and 1991 onward as wet phase by Guhathakurta and Rajeevan (2006) in National Climate Centre (NCC) report. A novel approach was adopted for analyzing the consistency of HW and CW. The frequency approach of each grid data was applied for HW and CW consistency mapping. The intensity of the same was measured by developing a new index multiplying consistency and frequency. This

approach and attempt to show the long-term average extreme temperature covering the entire India is new. The study explored that the average long-term extreme temperature in the wet phase is quite less than in the dry phase. Along with its novelty part, the scope of further research is needed to be mentioned. The study compared the extreme temperature condition based on two phases. Therefore, averaging the situation the Moving average approach in each phase could help to detect the specific extreme years.

Spatial mapping and analyzing the spatial trends of extreme temperature hot spots, cold spots, HW, and CW are of immense importance for designing priority basis spatial level planning. WMO (2022) sketched a conceptual framework of the impact of extreme temperature events. Increasing drought events, degradation of fish habitat, fish yield, ice melting, a decrease of wheat yield, increasing power shortage, heat stroke events, etc. CW has also some adverse impacts on the environment, health, and economy (Birthal et al., 2021). A wider part of northwest India was identified where the co-existence of both the high-intensity HW and CW are found. It does mean that the region is both ecologically and economically susceptible. HW and CW matrix map in this context is very useful from the planning point of view.

Conclusion

Spatial pattern analysis revealed that statistically significant (at 95% and 99% levels) hot-spot (maximum 1-year, 7-year, and 30-year) were found in the north western and central parts of India. The spatial extent of the 1-year hot spot was found more extensive than 7-year and 30-year in both the phases. A highly significant hot-spot area was observed squeezed over the recent phase. Cold-spot areas of winter time minimum temperature were recorded in extreme northern and north western parts of India. These hot-spot areas of maximum temperature (summer season) and cold-spot areas of minimum temperature (winter season) were also found susceptible to HW and CW respectively. HW consistently occurs over 60-65% geographical area covering north-western, central India, however, high-intensity HW (Greater than 10%) is confined within five major patches of this part covering only 27.72% geographical area. Intensification and extension of CW-prone areas were identified in the North-western Indian tract. CW intensity was found very high in the northern extreme of J & K and relatively high (10-19%) in north-western India in phase 1. While the frequency and intensity of CW in J & K declined to <30% and the north western tract was increased to 13-26.34%. CW with >10% frequency and intensity were extended towards the east in the continuity of its previous areal extent. About 46% of the area over Northwestern and Central

India is characterized by both highly consistent (consistency level: >0.67) HW and CW in 1991-2020. High-intensity HW and CW were found in the Delhi region and parts of Rajasthan covering only 11.26% area of the total area and phase-wise change is not significant, Areal extent of 5-day consecutive HW and CW co-existence is lesser than 2-day.

The finding of the study not only explored the areas of HW and CW-prone areas separately. Moreover, mapping the co-existence of high-intensity HW and CW is crucial from a vulnerability point of view. The regions' experiences co-existence of different intensity HW and CW requires different forms of planning implementation. The findings of this study would be instrumental for exposure, sensitivity analysis, and building adaptive capacity and accordingly designing adaptable planning.

Statements & Declarations

Ethical Approval

Not applicable

Consent to Participate

Not applicable

Consent to Publish

Not applicable

Authors Contributions

All the authors contributed to the study's conception and design. Conceptualization; Methodology designing; Supervision; editing and reviewing and writing of original draft were performed by Swades Pal and Priyanka Das. Data curation; investigation; formal analysis were performed by Rajesh Sarda and Doli Halder. All the authors read and approved the final manuscript.

Funding

No funds were received for this study.

Competing Interests

The authors declare that they have no competing interests

Availability of data and materials

The datasets used and/or analyzed during the current study are available from the corresponding author on reasonable request.

Acknowledgments

For this study, we would like to extend our gratitude to IMD for providing grid-level maximum and minimum temperature data.

References

Akhila, R.S., Kuttippurath, J., Balan Sarojini, B., Chakraborty, A. and Rahul, R., 2022. Observed tropical cyclone-driven cold wakes in the context of rapid warming of the Arabian Sea. *Journal of Operational Oceanography*, pp.1-16.

Arblaster, J.M. and Alexander, L.V., 2012. The impact of the El Niño-Southern Oscillation on maximum temperature extremes. *Geophysical Research Letters*, *39*(20).

Azhar, G., Saha, S., Ganguly, P., Mavalankar, D. and Madrigano, J., 2017. Heat wave vulnerability mapping for India. *International journal of environmental research and public health*, *14*(4), p.357.

Azhar, M.F., Qadir, I., Shehzad, M.M. and Jamil, A., 2022. Changing Climate Impacts on Forest Resources. In *Building Climate Resilience in Agriculture* (pp. 111-130). Springer, Cham.

Bakhsh, K., Rauf, S. and Zulfiqar, F., 2018. Adaptation strategies for minimizing heat wave induced morbidity and its determinants. *Sustainable cities and society*, *41*, pp.95-103.

Bedekar, V.C., Dekate, M.V. and Banerjee, A.K., 1974. Heat and cold waves in India. *India Meteorological Department Forecasting Manual*, *4*, p.63.

Birthal, P.S., Hazrana, J. and Negi, D.S., 2021. Impacts of climatic hazards on agricultural growth in India. *Climate and Development*, *13*(10), pp.895-908.

Budhathoki, N.K., Paton, D., Lassa, J.A., Bhatta, G.D. and Zander, K.K., 2020. Heat, cold, and floods: exploring farmers' motivations to adapt to extreme weather events in the Terai region of Nepal. *Natural Hazards*, *103*(3), pp.3213-3237.

Cai, W., Santoso, A., Collins, M. *et al.* Changing El Niño–Southern Oscillation in a warming climate. *Nat Rev Earth Environ* **2,** 628–644 (2021). https://doi.org/10.1038/s43017-021-00199-z

Chakraborty, D., Sehgal, V.K., Dhakar, R., Ray, M. and Das, D.K., 2019. Spatio-temporal trend in heat waves over India and its impact assessment on wheat crop. *Theoretical and Applied Climatology*, *138*(3), pp.1925-1937.

Change, I.C., 2013. The physical science basis.

673 Coumou, D. and Rahmstorf, S., 2012. A decade of weather extremes. *Nature climate*
674 *change*, *2*(7), pp.491-496.

675 Dar, J. and Dar, A.Q., 2022. Dominant patterns of seasonal precipitation variability in
676 association with hydrological extremes over the North-west Himalayas. *Environmental*
677 *Science and Pollution Research*, pp.1-14.

678 Das, P.K., Podder, U., Das, R., Kamalakannan, C., Rao, G.S., Bandyopadhyay, S. and Raj,
679 U., 2020. Quantification of heat wave occurrences over the Indian region using long-term
680 (1979–2017) daily gridded (0.5°× 0.5°) temperature data—a combined heat wave index
681 approach. *Theoretical and Applied Climatology*, *142*(1), pp.497-511.

682 Dhorde, A.G., Korade, M.S. and Dhorde, A.A., 2017. Spatial distribution of temperature
683 trends and extremes over Maharashtra and Karnataka States of India. *Theoretical and Applied*
684 *Climatology*, *130*(1), pp.191-204.

685 Drakes, O. and Tate, E., 2022. Social vulnerability in a multi-hazard context: a systematic
686 review. *Environmental Research Letters*.

687 Dubey, A.K. and Kumar, P., 2022. Future projections of heatwave characteristics and
688 dynamics over India using a high-resolution regional earth system model. *Climate Dynamics*,
689 pp.1-19.

690 Feng, R., Yu, R., Zheng, H. and Gan, M., 2018. Spatial and temporal variations in extreme
691 temperature in Central Asia. *International Journal of Climatology*, *38*, pp.e388-e400.

692 Findell, K.L., Berg, A., Gentine, P., Krasting, J.P., Lintner, B.R., Malyshev, S., Santanello,
693 J.A. and Shevliakova, E., 2017. The impact of anthropogenic land use and land cover change
694 on regional climate extremes. *Nature communications*, *8*(1), pp.1-10.

695 Guhathakurta, P. and Rajeevan, M., 2006. Trends in the rainfall pattern over India. NCC
696 research report (report no. 2/2006), National Climate Centre (NCC).

697 Habeeb, D., Vargo, J. and Stone, B., 2015. Rising heat wave trends in large US
698 cities. *Natural Hazards*, *76*(3), pp.1651-1665.

699 Kenyon, J. and Hegerl, G.C., 2008. Influence of modes of climate variability on global
700 temperature extremes. *Journal of Climate*, *21*(15), pp.3872-3889.

Kumar, A. and Singh, D.P., 2021. Heat stroke-related deaths in India: An analysis of natural causes of deaths, associated with the regional heatwave. *Journal of thermal biology*, *95*, p.102792.

Kumar, P., Rai, A., Upadhyaya, A. and Chakraborty, A., 2022. Analysis of heat stress and heat wave in the four metropolitan cities of India in recent period. *Science of The Total Environment*, *818*, p.151788.

Kumar, P., Mishra, A.K., Dubey, A.K., Javed, A., Saharwardi, M., Kumari, A., Sachan, D., Cabos, W., Jacob, D. and Sein, D.V., 2022. Regional earth system modelling framework for CORDEX-SA: an integrated model assessment for Indian summer monsoon rainfall. *Climate Dynamics*, pp.1-20.

Lesk, C., Rowhani, P. and Ramankutty, N., 2016. Influence of extreme weather disasters on global crop production. *Nature*, *529*(7584), pp.84-87.

Lorenz, R., Jaeger, E.B. and Seneviratne, S.I., 2010. Persistence of heat waves and its link to soil moisture memory. *Geophysical Research Letters*, *37*(9).

Mahdi, S.S. and Dhekale, B.S., 2016. Long term climatology and trends of heat and cold waves over southern Bihar, India. *Journal of Earth System Science*, *125*(8), pp.1557-1567.

Malik, P., Bhardwaj, P. and Singh, O., 2020. Distribution of cold wave mortalities over India: 1978–2014. *International Journal of Disaster Risk Reduction*, *51*, p.101841.

McCarl, B.A., 2013. Climate change and food security.

McCormick, S., 2012. Extreme heat and cold. In *The Routledge Handbook of Hazards and Disaster Risk Reduction* (pp. 269-280). Routledge.

Miller, A.A., 2019. *Climatology*. Routledge.

Mishra, P.K., 2017. Socio-economic impacts of climate change in Odisha: issues, challenges and policy options. *Journal of Climate Change*, *3*(1), pp.93-107.

Murari, K.K., Sahana, A.S., Daly, E. and Ghosh, S., 2016. The influence of the El N iño Southern Oscillation on heat waves in India. *Meteorological Applications*, *23*(4), pp.705-713.

Naveena, N., Satyanarayana, G.C., Rao, K.K., Umakanth, N. and Srinivas, D., 2021. Heat wave characteristics over India during ENSO events. *Journal of Earth System Science*, *130*(3), pp.1-16.

730 Ord, J.K. and Getis, A., 1995. Local spatial autocorrelation statistics: distributional issues and
731 an application. *Geographical analysis*, *27*(4), pp.286-306.

732 Pai, D.S., Srivastava, A.K. and Nair, S.A., 2017. Heat and cold waves over India.
733 In *Observed climate variability and change over the Indian Region* (pp. 51-71). Springer,
734 Singapore.

735 Pal, S. and Ziaul, S.K., 2017. Detection of land use and land cover change and land surface
736 temperature in English Bazar urban centre. *The Egyptian Journal of Remote Sensing and*
737 *Space Science*, *20*(1), pp.125-145.

738 Panda, D.K., Mishra, A., Kumar, A., Mandal, K.G., Thakur, A.K. and Srivastava, R.C., 2014.
739 Spatiotemporal patterns in the mean and extreme temperature indices of India, 1971–
740 2005. *International Journal of Climatology*, *34*(13), pp.3585-3603.

741 Panda, D.K., AghaKouchak, A. and Ambast, S.K., 2017. Increasing heat waves and warm
742 spells in India, observed from a multiaspect framework. *Journal of Geophysical Research:*
743 *Atmospheres*, *122*(7), pp.3837-3858.

744 Parliari, D., Giannaros, C. and Keppas, S., 2022. Assessment of Heat and Cold Waves
745 Phenomena and Impacts on Environment. In *Extremes in Atmospheric Processes and*
746 *Phenomenon: Assessment, Impacts and Mitigation* (pp. 141-167). Springer, Singapore.

747 Perkins, S.E., 2015. A review on the scientific understanding of heatwaves—Their
748 measurement, driving mechanisms, and changes at the global scale. *Atmospheric*
749 *Research*, *164*, pp.242-267.

750 Pingale, S.M., Khare, D., Jat, M.K. and Adamowski, J., 2014. Spatial and temporal trends of
751 mean and extreme rainfall and temperature for the 33 urban centers of the arid and semi-arid
752 state of Rajasthan, India. *Atmospheric Research*, *138*, pp.73-90.

753 Praveen, B., Talukdar, S., Mahato, S., Mondal, J., Sharma, P., Islam, A.R.M. and Rahman,
754 A., 2020. Analyzing trend and forecasting of rainfall changes in India using non-parametrical
755 and machine learning approaches. *Scientific reports*, *10*(1), pp.1-21.

756 Rajkumar, R., Shaijumon, C.S., Gopakumar, B. and Gopalakrishnan, D., 2021. Recent
757 patterns of extreme temperature events over Tamil Nadu, India. *Climate Research*, *84*, pp.75-
758 95.

759 Ranagalage, M., Estoque, R., Zhang, X., & Murayama, Y. (2018). Spatial changes of urban
760 heat island formation in the Colombo District, Sri Lanka: Implications for sustainability
761 planning. *Sustainability*, *10*(5), 1367.
762 .

763 Rao, Y.P. and Srinivasan, V., 1969. Discussion of typical synoptic weather situation: winter
764 western disturbances and their associated features. *Indian Meteorological Department:*
765 *Forecasting Manual Part III*.

766 Ratnam, J.V., Behera, S.K., Ratna, S.B., Rajeevan, M. and Yamagata, T., 2016. Anatomy of
767 Indian heatwaves. *Scientific reports*, *6*(1), pp.1-11.

768 Raymond, C., Horton, R.M., Zscheischler, J., Martius, O., AghaKouchak, A., Balch, J.,
769 Bowen, S.G., Camargo, S.J., Hess, J., Kornhuber, K. and Oppenheimer, M., 2020.
770 Understanding and managing connected extreme events. *Nature climate change*, *10*(7),
771 pp.611-621

772 Revadekar, J.V., Kothawale, D.R., Patwardhan, S.K., Pant, G.B. and Rupa Kumar, K., 2012.
773 About the observed and future changes in temperature extremes over India. *Natural*
774 *hazards*, *60*(3), pp.1133-1155.

775 Rohini, P., Rajeevan, M. and Srivastava, A.K., 2016. On the variability and increasing trends
776 of heat waves over India. *Scientific reports*, *6*(1), pp.1-9.

777 Russo, S., Sillmann, J. and Fischer, E.M., 2015. Top ten European heatwaves since 1950 and
778 their occurrence in the coming decades. *Environmental Research Letters*, *10*(12), p.124003.

779 Sanjay, J., Revadekar, J.V., RamaRao, M.V.S., Borgaonkar, H., Sengupta, S., Kothawale,
780 D.R., Patel, J., Mahesh, R., Ingle, S., AchutaRao, K. and Srivastava, A.K., 2020. Temperature
781 changes in India. In *Assessment of climate change over the Indian Region* (pp. 21-45).
782 Springer, Singapore.

783 Sarda, R. and Das, P., 2018. Monitoring changing trends of water presence state in the major
784 manmade reservoirs of Mayurakshi river basin, eastern India. *Spatial Information*
785 *Research*, *26*(4), pp.437-447.

786 Seneviratne, S., Nicholls, N., Easterling, D., Goodess, C., Kanae, S., Kossin, J., Luo, Y.,
787 Marengo, J., McInnes, K., Rahimi, M. and Reichstein, M., 2012. Changes in climate
788 extremes and their impacts on the natural physical environment.

789 Serrano-Notivoli, R., Lemus-Canovas, M., Barrao, S., Sarricolea, P., Meseguer-Ruiz, O. and
790 Tejedor, E., 2022. Heat and cold waves in mainland Spain: Origins, characteristics, and
791 trends. *Weather and Climate Extremes*, p.100471.

792 Sillmann, J., Kharin, V.V., Zhang, X., Zwiers, F.W. and Bronaugh, D., 2013. Climate
793 extremes indices in the CMIP5 multimodel ensemble: Part 1. Model evaluation in the present
794 climate. *Journal of Geophysical Research: Atmospheres*, *118*(4), pp.1716-1733.

795 Singh, S., Mall, R.K. and Singh, N., 2021. Changing spatio-temporal trends of heat wave and
796 severe heat wave events over India: An emerging health hazard. *International Journal of*
797 *Climatology*, *41*, pp.E1831-E1845.

798 Smid, M., Russo, S., Costa, A.C., Granell, C. and Pebesma, E., 2019. Ranking European
799 capitals by exposure to heat waves and cold waves. *Urban Climate*, *27*, pp.388-402.

800 Solomon, S., Qin, D., Manning, M., Chen, Z., Marquis, M., Averyt, K., Tignor, M. and
801 Miller, H., 2007. Climate change 2007: The scientific basis. Contribution of Working Group I
802 to the fourth assessment report of the Intergovernmental Panel on Climate
803 Change. *Cambridge University Press, Cambridge, UK*, *996*.

804 Sonali, P. and Kumar, D.N., 2013. Review of trend detection methods and their application to
805 detect temperature changes in India. *Journal of Hydrology*, *476*, pp.212-227.

806 Srivastava, A.K., Rajeevan, M. and Kshirsagar, S.R., 2009. Development of a high resolution
807 daily gridded temperature data set (1969–2005) for the Indian region. *Atmospheric Science*
808 *Letters*, *10*(4), pp.249-254.

809 Stillman, J.H., 2019. Heat waves, the new normal: summertime temperature extremes will
810 impact animals, ecosystems, and human communities. *Physiology*, *34*(2), pp.86-100.

811 Subash, N., Singh, S.S. and Priya, N., 2013. Observed variability and trends in extreme
812 temperature indices and rice–wheat productivity over two districts of Bihar, India—a case
813 study. *Theoretical and applied climatology*, *111*(1), pp.235-250.

814 Tran, D.X., Pla, F., Latorre-Carmona, P., Myint, S.W., Caetano, M. and Kieu, H.V., 2017.
815 Characterizing the relationship between land use land cover change and land surface
816 temperature. *ISPRS Journal of Photogrammetry and Remote Sensing*, *124*, pp.119-132.

817 Weilnhammer, V., Schmid, J., Mittermeier, I., Schreiber, F., Jiang, L., Pastuhovic, V., Herr,
818 C. and Heinze, S., 2021. Extreme weather events in europe and their health consequences–A

systematic review. *International Journal of Hygiene and Environmental Health*, *233*, p.113688.

Wolf, T. and McGregor, G., 2013. The development of a heat wave vulnerability index for London, United Kingdom. *Weather and Climate Extremes*, *1*, pp.59-68.

Supplementary Files

This is a list of supplementary files associated with this preprint. Click to download.

- SupplementaryMaterials.docx